

Entanglement-assisted authenticated BB84 protocol

Pol Julià Farré*, Vladlen Galetsky†, Soham Ghosh†, Janis Nötzel†, Christian Deppe*

*Technical University of Braunschweig, Braunschweig, Germany

†Technical University of Munich, Munich, Germany

Email: *pol.julia-farre@tu-braunschweig.de, †vladlen.galetsky@tum.de,

†soham.ghosh@tum.de, †janis.noetzel@tum.de, *christian.deppe@tu-braunschweig.de

Abstract—This work delivers a novel user-server authentication procedure exploiting the features of maximally entangled pairs in both an idealistic noiseless scenario and a moderately noisy one. Additionally, we leverage the specific features of our design, which are conveniently suited for inlaying it into the well known BB84 quantum communication protocol. We first define a trivial extension of our initial proposal allowing for such task (symmetric scheme) to then come up with what we denote as asymmetric scheme, better matching practicality.

Furthermore, a realistic simulation of the user-server authentication protocol has been achieved by employing a noisy model for both transmission and storage, the latter relying on cavity-enhanced atomic-frequency comb (AFC) memories. While in a noiseless scenario our proposal is ensured to be airtight, considering a certain degree of noise poses a challenge when aiming to actually implement it. We have implemented a deep neural network to distinguish legitimate users from forgery attempts, outperforming a mere statistical approach designed for the same task. Such method achieved a success rate of 0.75 with storage times of $1 \mu\text{s}$ and a user-server distance of 10 km.

Index Terms—Authenticated QKD, BB84, realistic simulation, AFC memory, entanglement-assisted authentication, secret pre-sharing.

I. INTRODUCTION

Quantum key distribution (QKD) emerged as a post-quantum solution to the security threat posed by Shor’s algorithm, which would compromise the RSA cryptosystem if sufficiently large and efficient quantum computers were developed. Following the seminal proposals [1], which relies on Heisenberg’s uncertainty principle, and [2], which utilizes entanglement, numerous variations have been developed to enhance security and practicality. The review in [3] and the comprehensive survey in [4] outline the state of the art in QKD and its evolution over the past decades. In particular, continuous variable QKD schemes, as discussed in [5], represent a significant departure from the original protocols and have become prominent in recent research.

Before delving into the core content of this article, it is essential to introduce the concept of authentication schemes, which ensure that an entity claiming to be a specific party is indeed who he/she claims to be. Authentication can be based on something the entity *has* (token-based authentication), something the entity *knows* (passwords, pre-shared keys, etc.), or something the entity *is* (biometrics-based authentication). A comprehensive review of quantum authentication methods

is available in [6], highlighting recent advancements such as quantum physical unclonable functions (QPUFs) [7]–[9].

Given the importance of both QKD and authentication, it is crucial to recognize their interconnection. While often eluded in the literature, QKD relies on the assumption that the parties involved are securely authenticated. This authentication can be achieved through either classical or quantum methods. Our work, among other contributions subsequently listed, serves as an example of the latter, integrating quantum authentication techniques to enhance the security framework of QKD systems. Mainly, we introduce a new level of security by pre-sharing entanglement, addressing a vulnerability in the state of the art [10], [11], where identity forgery can be performed only by stealing classical information. In our approach, maximally entangled pairs halves are embedded in the BB84 QKD protocol for authentication, making the theft of quantum systems a necessity for impersonation attacks.

Our contributions

In this article, we present a new authentication protocol leveraging the intrinsic entanglement properties exhibited by two-qubit systems (see Section III). The architecture of this protocol enables one-party identity authentication under noiseless assumptions. In Section IV, we demonstrate how our protocol can be further exploited by embedding it within the well-known BB84 QKD protocol [1], utilizing what we define as symmetric and asymmetric schemes. These proposals, contrasted with respect to the state of the art [10], [11] in Section IV-D, introduce novel authenticated communication procedures that provide computational security under specific pre-sharing assumptions, which are detailed in our description.

We approach the problem of authentication in a noisy scenario as a binary data classification task. To address it, we propose two methods: a trivial approach and a machine learning algorithm (see Sec III-B). In Section V, we simulate a realistic user-server authentication protocol to quantify the performance of our data classifiers. In Section V-A1, we model an optical channel incorporating dephasing and decoherence noise, and taking dark counts and detection efficiencies into account. For storage, we consider cavity-enhanced AFC memories, reviewing their state of the art in Section V-A2.

By highlighting the evolution of key performance metrics for the required hardware over the past years, we acknowl-

edge the potential of our designs and implicitly state future perspectives based on this progress.

II. PRELIMINARIES

In this section, we first provide a brief glossary of key terms related to security. Following that, we establish the notation that is used throughout the article.

A. Glossary

Let us start by defining a crucial concept in the field of computational security:

Definition 1. Security parameter:

The security parameter of a scheme is a scalar quantity intrinsically defined within it, i.e., with a physical meaning with regards to the required setup. Negligibility is defined towards this parameter as being any quantity asymptotically decreasing faster than any inverse polynomial of it.

Furthermore, two crucial definitions in the realm of logic are as follows: a statement is considered valid if it is provable (completeness property), and only a provable statement is valid (soundness property). These definitions have been adopted by the field of information science to define what constitutes a secure scheme [12]. Accordingly, we adapt these two properties to the specific logic system defined by authentication protocols, in a general context:

Definition 2. Completeness:

An actual user of the server is not accepted when being authenticated with a negligible probability.

Definition 3. Soundness:

An attempt to forge the user is accepted when being authenticated with a negligible probability.

Definition 4. Authentication protocol security:

A secure authentication protocol is defined as being that one owning both: completeness and soundness.

Finally, we precisely define the notion of an adversary.

Definition 5. Adversary:

Entity aiming to forge the identity of the user within the context of an authentication protocol.

The limitations on the power of the adversary party are crucial and must be clearly acknowledged, in order for the displayed security proofs to be meaningful. In our considered scenarios, the assumptions made on any adversary are that

- 1) theft of quantum systems owned by the actual party being authenticated is ruled out.
- 2) tampering with the sent quantum systems assisting the authentication is, instead, allowed.

The first consideration becomes apparent in our security proofs, where such constraint is actively exploited. Regarding the second consideration, we assert *intercept-resend attack* resistance for our schemes. Having that those so called jamming attacks [13] may compromise the completeness of our proposals, but not their soundness.

B. Notation

During the whole paper, the Dirac notation is used to represent quantum states. In addition, quantum gates are denoted as capital letters.

The following definitions serve us as examples of such convention and allow us to present 3 gates that appear in this work:

We introduce the well-known unitary operators X and Z (Pauli- X and Pauli- Z , respectively) by describing their action onto the computational basis of $\mathcal{H} = \mathbb{C}^2$ as

$$X |j\rangle = |j \oplus 1\rangle \quad \& \quad Z |j\rangle = (-1)^j |j\rangle, \quad (1)$$

and we analogously define the Hadamard gate, H , as

$$H |j\rangle = \frac{1}{\sqrt{2}} \left(|0\rangle + (-1)^j |1\rangle \right), \quad (2)$$

where $j = 0, 1$.

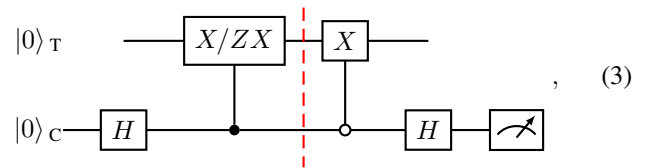
As a final remark, all quantum circuits shown are in agreement with the common formalism used in quantum computation. Hence, their time axis runs from left to right, as well as quantum gates are enclosed within boxes. Measurements are, in all of the cases considered, taken at the very end of the circuit and always assumed to happen in the computational basis.

III. CX/CZX AUTHENTICATION PROTOCOL

We now present our proposed entanglement-assisted authentication protocol. Initially, we define a noiseless version of the protocol, followed by a discussion on its adaptation to a noisy scenario.

A. Noiseless protocol definition

The CX/CZX authentication protocol starts with the first stage of the following quantum circuit



On the left side of the red dashed line, the generation stage occurs. Subsequently, the control (C) and target (T) registers are separated. Next, the second part of the quantum circuit is executed, representing the verification stage.

where the controlled gates appearing are nothing but the controlled versions of either X or ZX , acting on the target qubit, T, when the control system, C, is on state "1" (black circle) or "0" (white circle).

Following this initial phase, the target system is transferred to the user, who retains it until the verification stage, i.e., the second part described in Eq. (3), occurs.

This circuit is executed λ times, where λ represents the security parameter of the protocol. At each iteration, a choice

is made between applying CX or CZX . The user is then authenticated as a legitimate one if a "0" is consistently obtained at the control register whenever CX was utilized, and a "1" is obtained in all other cases.

a) *Completeness*: The probability of accepting the user is exactly equal to 1 in a *noiseless scenario* (see Proposition 1).

b) *Soundness*: The probability for an attacker to produce a successful forgery, p_{f_A} , decreases exponentially with λ , the security parameter of the scheme.

More specifically (see Proposition 2),

$$p_{f_A} = \frac{1}{2^\lambda} \quad (4)$$

B. Noise-adapted definition of the protocol

Due to the inevitability of errors arising from quantum gates, transmission and storage, our previous definition for the "user acceptance condition" lacks robustness. Therefore, we propose two alternative approaches with the objective of devising a more suitable protocol for a practical implementation.

Acceptance condition a): According to this definition, the user is reckoned as an actual one as long as the rate r_{01} of correctly matching binary outcomes "0"/"1" fulfills

$$r_{01} \geq \mu. \quad (5)$$

For some $\mu > \frac{1}{2} + \frac{1}{\sqrt{2\lambda}}$, in order to distinguish the actual user from a forgery attempt.

The described protocol is no longer guaranteed to be neither sound nor complete. That is, firstly, the probability for an attacker to be accepted decreases polynomially in λ , and, thus, cannot be reckoned as being negligible anymore.

Specifically, an attacker successfully passes verification with a probability p_{f_B} , fulfilling (see Proposition 3)

$$p_{f_B} \leq \frac{1}{2\lambda} \frac{1}{\left(\mu - \frac{1}{2}\right)^2}, \quad (6)$$

which is well defined and establishes a non-trivial bound due to the specified constraint in the choice of μ .

On the other hand, whether legitimate users will be accepted or not is now dependent on the noisy hardware implementation.

Acceptance condition b): A binary string S needs to be created, where each position is filled with a "1" if the outcome matches the expected one and a "0" otherwise. This string is then processed by a deep neural network (DNN) [14] specialized in solving the binary classification problem. The DNN determines whether the outcomes correspond to a legitimate user or a forgery attempt.

The motivation for using a machine learning algorithm for this task is that the string S generated by a legitimate user exhibits a much more complex structure compared to those generated by malicious parties. The first proposed *user acceptance condition* only captures that the mean of this string is generally higher than $\frac{1}{2}$ for legitimate users, but it does not

account for the fact that the initial inputs are more likely to match the expectation better than the later ones, where noise has a greater impact.

IV. CX/CZX AUTHENTICATION PROTOCOL EMBEDDED IN THE BB84 SCHEME

In this section, we begin by outlining the BB84 QKD protocol [1]. We then propose two methods for integrating in it the authentication scheme we have defined. Additionally, we discuss how these proposals compare to the current state of the art in QKD authentication, with [10] serving as the primary related work.

A. BB84 protocol: overview

a) *Secret key generation and encoding*: The BB84 protocol defines two communication parties: Alice, the sender, and Bob, the receiver. Alice randomly generates a secret binary key, which she aims to communicate to Bob to enable secure encoding of a subsequent message. Each bit of this key is encoded in the state of a qubit. Bits with the value "0" are encoded in either the state $|0\rangle$ or the state $|+\rangle \equiv \frac{1}{\sqrt{2}}(|0\rangle + |1\rangle)$, with equal probability. Conversely, bits with the value "1" are encoded in either the state $|1\rangle$ or the state $|-\rangle \equiv \frac{1}{\sqrt{2}}(|0\rangle - |1\rangle)$, also with equal probability. This encoding strategy is commonly referred to as encoding a bit in the Z or X basis, respectively.

b) *Key transmission and decoding*: After the secret key has been encoded in a quantum system, Alice sends it to Bob, who must measure each qubit either in the Z or X basis out of a uniformly random distributed choice. From this set of measurements he obtains a binary key. Following this action, Alice publicly acknowledges her choice of bases and, in those qubits where the basis coincides, noiseless quantum theory ensures coincidence between the bits owned at both sides. That allows for a creation of a shared secret key of an expected size being half of the length of the originally sent bitstring.

c) *Information reconciliation and privacy amplification*: Although noiseless quantum theory validates the described protocol and allows for a rigorous proof of its security [15], real-world physical scenarios involve errors from multiple sources, resulting in noisy systems. The authors of [1] acknowledged this and proposed the information reconciliation [16] and privacy amplification [17] algorithms which, when applied sequentially and under certain constraints on the quantum bit error rate (QBER) [11]¹, ensure a functional QKD protocol in practical settings.

d) *Eavesdropping resilience*: A desired property of the protocol we are describing is its ability to easily detect a *Man-in-the-Middle attack* [18]. This can be achieved by having Alice and Bob split the initially generated key into two sets immediately after acknowledging the choice of bases. One set continues with the QKD protocol, while the other, comprising a small portion of the total key, is used to check for high correlation rates. Such high correlation is achieved **only if no**

¹The cited reference specifies that a maximum QBER of approximately 11% is required.

eavesdropper intercepted and acquired information from the transmitted qubits [19].

B. Our proposals

We now outline the steps required to implement two different authentication procedures embedded within the BB84 protocol (see Fig. 1). The first procedure is labeled as symmetric because a bidirectional quantum channel allows both Alice and Bob to authenticate each other using the protocol defined in Section III-B. The second proposal involves an additional action on Bob's side, enabling both parties to authenticate each other using a unidirectional quantum channel. This scheme better aligns with the hardware requirements of the BB84 protocol, but, in order to achieve this, the symmetry of the protocol is broken. That is, the authentication process differs fundamentally depending on the party involved.

1) Symmetric scheme:

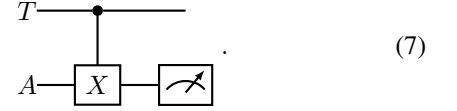
- **1st step:** Our proposal starts with an additional constraint compared to those of the BB84 protocol: *Alice and Bob must coincide spatially and temporally before initiating the QKD protocol*, or at least before a series of n QKD protocols commence.
- **2nd step:** We describe the most general scenario, involving a sequence of n QKD protocols. In this case, Alice and Bob require $4n\lambda$ qubits, with 4λ allocated for each QKD round. These undergo the first stage as described in Eq. 3, operating in pairs and always applying CX , thereby consistently yielding an expected outcome of "0" at verification.
- **3rd step:** Alice and Bob secretly agree in a string K of λ integer values, encoding a set of positions between the string of qubits devoted to distribute a secretly shared key. This special requirement falls into what in the literature is known as *secret pre-sharing*.
- **4th step:** Alice stores $2n\lambda$ target qubits, while Bob carries $2n\lambda$ control qubits.
- **5th step:** At each protocol, Alice embeds λ of her target qubits, now also referred to as "authenticating (AU) qubits", within the string of qubits used for QKD, and positioned at the agreed positions. Additionally, Bob sends Alice λ of his control (AU) qubits, which are entangled with the ones retained by Alice.
- **6th step:** Both parties can now authenticate each other using the scheme described in Section III-B, by defining $S \equiv S_A$ at Bob's side and $S \equiv S_B$ at Alice's.

2) Asymmetric scheme:

- **1st step:** The asymmetric scheme also requires Alice and Bob to spatially coincide in time before the QKD protocol begins, or at least before a series of n QKD protocols commence.
- **2nd step:** Alice and Bob are provided with $4n\lambda$ qubits, with 4λ allocated for each QKD round. All these qubits undergo the first stage described in Eq. 3. Additionally, a binary key F , owned only by Alice, encodes the choices

made during each circuit run ($CX("0")/CZX("1")$), which must be uniformly random.

- **3rd step:** Alice and Bob secretly agree on a string K consisting of 2λ integer values, encoding positions within the qubit string at each QKD round, between the qubits used to distribute a secretly shared key.
- **4th step:** Similar to the symmetric case, Alice stores the entire set of $2n\lambda$ target qubits, while Bob retains the $2n\lambda$ control qubits.
- **5th step:** At each protocol, Alice embeds 2λ of her target qubits, now comprising the entire set of AU qubits, within the qubit string used for QKD, and at the agreed positions.
- **6th step:** Bob divides his 2λ entangled pairs into two halves. The first half is sent through the second stage described in Eq. 3, enabling Alice to verify Bob's identity by requesting him to publicly communicate the classical outcomes obtained at the control registers (see Section III-B), aggregated into a bitstring F' .
Onto each of the remaining entangled pairs, Bob applies the circuit



Acceptance condition a)

According to this definition, Bob requires a rate r_0 of outcomes with the result "0" to be greater than $\mu > \frac{1}{2} + \frac{1}{\sqrt{2\lambda}}$. This criterion allows him to determine that the identity of Alice is being forged with a probability p_{fc} , satisfying (see Proposition 3)

$$p_{fc} \leq \frac{1}{2\lambda} \frac{1}{\left(\mu - \frac{1}{2}\right)^2}. \quad (8)$$

Similarly, Alice can verify Bob's identity by requiring a ratio r_{01} of coincidence between F and F' to be above the same threshold, μ .

Acceptance condition b)

Alternatively, the neural network method mentioned in our user-server protocol can be employed again to authenticate both parties, leveraging the structure of the noise affecting the authenticating qubits, particularly the time arrow.

To achieve this, Bob and Alice need to create a string, S_A and S_B respectively, containing a "1" at positions where outcomes match expectations and a "0" otherwise. The classifier then determines whether to accept or reject the string created by each party.

C. Desirable properties

We now display the strengths of our new schemes:

- Our proposals provide a method for authenticating both parties involved in a specific and widely used QKD scheme. The security of the protocol can be guaranteed

in a noiseless scenario (see Proposition 4) by requiring a perfect match between F and F' , and by ensuring that Bob obtains an outcome of "0" in all instances when running Eq. (7). However, in the presence of noise, we address the authentication task through either statistical analysis or a neural network scheme.

- The authenticating qubits sent by Alice can also be used to detect a *Man-in-the-Middle attack*. Successful authentication requires no tampering with the authenticating qubits, which are indistinguishable from those transmitted for QKD purposes. If successful authentication does not occur, the protocol is aborted. Thus, the authenticating qubits not only serve the purpose of authentication but also prevent the need to relinquish a small portion of the initial qubits intended for QKD immediately after the public sharing of bases choice.

D. Benchmarking

When dealing with message authentication codes (MACs) [20], or more specifically, with authenticated QKD [21], there is not a single metric allowing for a qualitative comparison between existing methods in the state of the art.

A ubiquitous trade-off in this field is the amount of pre-shared secrecy required which, at first glance, seems not feasibly avoidable. While providing a rigorous and trustworthy answer on whether pre-shared secrecy is always necessary or not remains a challenge [22], one of the most current and efficient ways of message authentication today involves the use of hash functions [23], which all require pre-shared secrecy [24], [25].

In [11], a classically authenticated QKD scheme without pre-shared secrecy requirements is proposed, but it relies on being assisted by the usage of pseudorandomness and efficient distinguishability from pure randomness. Additionally, it implicitly assumes the existence of an authenticated classical channel between the two parties.

Our contribution introduces two distinct quantum QKD authenticated protocols in which Bob and Alice are required to be gathered together in an initial stage, where pre-shared secrecy takes place before a sequence of n independent QKDs occurs.

We aim to highlight how our proposals represent a specific application of a one-party authentication protocol newly introduced in Section III. Although our schemes resemble the ideas from [10], we present a genuinely different authenticated QKD procedure with distinct hardware requirements and different derived theoretical properties. Mainly, we address eavesdropping detection using the authenticating qubits themselves and explicitly require the theft of quantum systems for the scheme to be compromised. In contrast, the proposal in [10] can be broken by the mere theft of classical information, while conveniently eliminating the need for entanglement generation. Thus, we believe that our work complements the cited authors and opens new lines of investigation in the realm of quantum authentication.

V. REALISTIC SIMULATION

A. Methods

In this section, we outline the methodology employed to simulate our user-server authentication protocol in a realistic scenario. The simulation adopts a shot-by-shot (photon-by-photon) approach, where a scheduler is implemented to monitor the local time of each photon at every stage of the simulation. This method enables the construction of a realistic storage and waiting times between user-server authentication stages. The noise model, accounting for transmission loss, storage efficiency and detection efficiency, yields the probability of a photon not being detected at each phase of our defined protocol.

The parameters characterizing our model are detailed in Table I, and all simulations described in this paper were parallelized [26] on a 2x Intel Xeon Platinum 8176 @ 2.1GHz processor.

At the start of our scheme, both the control and target registers are evolved using either the CX or the CZX gate. The expected gate and readout errors, along with qubit decoherence and dephasing times (T_1 and T_2), are derived from the calibration data of the IBM Brisbane quantum processor.

We are considering, at sides of both the server and the user, multiple AFC type memories [27], which couple with the radio frequency of the photon and do not require additional conversions as in the case of Nitrogen vacancy centers or transmon coupled cavities. As seen in the state of the art, the single mode AFC storage can achieve a maximum coherent storage time of an hour [28] by employing a zero first-order-Zeeman magnetic field and dynamical decoupling to protect the spin coherence with a fidelity of 96.4% [27], [29]. For multimode AFC memories, over 15 spacial \times 30 temporal modes [30] and 1060 temporal modes [31] have already been demonstrated, with lifetimes achieving 0.542 ms [32]. The dephasing time for AFC can achieve $T_2 = 300 \pm 30 \mu\text{s}$ experimentally, as seen in [33].

1) *Channel attenuation*: Considering a frequency of the source of $f_{\text{source}} = 33$ MHz [34], each photon is sent through an optical fiber channel. The wavelength of the source was chosen so that it could be compatible with AFC quantum memories with no additional frequency conversion losses, as demonstrated with erbium-doped crystal type AFC in [35]. The fiber loss channel is described by the single-photon transmission probability [36]

$$\eta_{\text{channel}} = 10^{-d\tau/10}, \quad (9)$$

with d being the transmission distance between the user and the server and $\tau = 0.17$ dBkm $^{-1}$ being the fiber attenuation with a refractive index of glass in the fiber of $r_{\text{glass}} = 1.44$.

Before storage, the photon is detected from the fiber optical channel and we consider a detection efficiency of $p_{\text{detect}} = 0.9$ [34].

The dark count probability follows the Poisson distribution [36]

TABLE I: Simulation parameters

Parameter	Value	Unit	Parameter	Value	Unit
Qubit decoherence time (T_1)	$2.2344 \cdot 10^2$	μs	Comb finesse (F)	$4 \cdot 10$	-
Qubit dephasing time (T_2)	$2.9535 \cdot 10^2$	μs	Comb absorption efficiency (α)	1.0	-
Reflectivity mirror 1 (R_1)	$9.6 \cdot 10^{-1}$	-	Comb FWHM linewidth (ϵ)	3.0	kHz
Reflectivity mirror 2 (R_2)	$9.9 \cdot 10^{-1}$	-	Number of photons Fig. 2/ Fig. 3 (2λ)	$10^3 / 2 \cdot 10^2$	-
Source frequency (f_{source})	$3.3 \cdot 10$	MHz	Detection efficiency (p_{detect})	$9.5 \cdot 10^{-1}$	-
Source wavelength	$1.550 \cdot 10^3$	nm	Fiber attenuation (τ)	$1.7 \cdot 10^{-1}$	dBkm $^{-1}$
Driven recovery time	$3.0 \cdot 10$	ns	C – T : CZX gate error	6.4×10^{-3}	-
Driven storage time	$3.0 \cdot 10$	ns	C – T : CX gate error	6×10^{-3}	-
Photon velocity in fiber	2.08×10^8	ms $^{-1}$	C: Hadamard gate error	1.48×10^{-4}	-
Dark count frequency (f_{dark})	$1.0 \cdot 10$	Hz	C: Readout error	2.16×10^{-2}	-

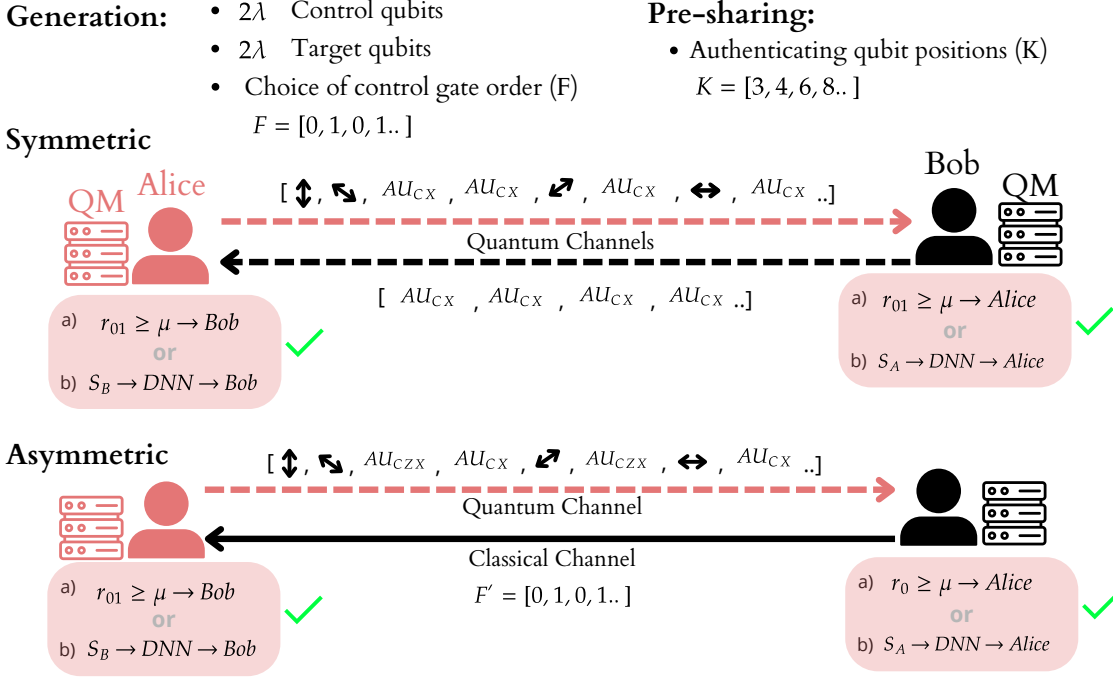


Fig. 1: The entanglement-assisted authenticated BB84 protocol comes in both symmetric and asymmetric versions, having the specifics of each protocol varying depending on whether acceptance condition a) or b) is chosen. $n = 1$ was selected for simplicity and QM refers to the quantum memory available at each side.

$$\eta_{\text{dark}} = 1 - e^{-t_w f_{\text{dark}}}, \quad (10)$$

with a capture window of the detector being $t_w = 25$ ns. f_{dark} is the frequency of dark counts, which has been experimentally determined to be approximately $f_{\text{dark}} \approx 10$ Hz [34]. This value has been used in our simulations.

2) *Quantum memory*: For the storage we consider a stark modulated AFC memory with an optical cavity from [29] and we make two assumptions:

- We use as many cavity-enhanced AFC memories as needed for the size of the quantum key, assuming we can extrapolate their storage-retrieval efficiency model to multimode quantum AFC memories.
- We choose the finesse F of the comb in accordance with the storage efficiency model described in [29]:

$$\eta_{\text{cav}} = \frac{4(\bar{\alpha}l)^2 e^{-2\bar{\alpha}l} (1 - R_1)^2 R_2 e^{-t^2 \bar{\epsilon}^2}}{(1 - \sqrt{R_1 R_2} e^{-\bar{\alpha}l})^4}, \quad (11)$$

where t is the storage time of the photon, $\bar{\alpha} = \frac{\alpha}{F} \sqrt{\frac{\pi}{4 \ln(2)}}$ is the effective absorption of the comb, α is the absorption coefficient of the comb peaks and l is the crystal length. $R_1 = 0.96$ and $R_2 = 0.99$ are the mirror reflectivities and $\bar{\epsilon} = \frac{2\pi\epsilon}{\sqrt{8 \ln(2)}}$ is related to the comb FWHM ϵ .

The storage and retrieval efficiency involves a trade-off when choosing F : higher absorption probability corresponds to a smaller F , while increasing F reduces dephasing during storage [37]. In our simulation we have opted for $F = 40$ and $\alpha l = 1$, with ϵ of 3 kHz and with negligible inter-cavity loss. Experimentally with $F_{\text{AFC}} = 5.8$ storage-retrieval efficiencies of $55 \pm 5\%$ [38] and 62% [27] were obtained for cavity coupled AFCs, but we expect that the parameters chosen for our

simulation may be achievable for AFC with persistent holes and with ϵ in the order of kHz in the near future [29]. Despite of its relevance, in the simulation we have not considered the dependence of the added atomic dephasing due to the change in comb finesse [39]. In Table II, we provide an overview of the main parameters from cavity enhanced AFC experiments developed through the past years.

For the simulation, we have considered an intrinsic efficiency of 100% to convert from kHz to telecom frequency, which may be achievable for single photons [40]. Moreover, we have considered driven storage and recovery times of 30 ns for each photon.

3) *DNN post-processing*: To adapt our user-server authentication protocol to noise, we have first introduced the parameter μ , which, under low noise assumptions and by setting it to be small enough, ensures that legitimate users are accepted with high probability. On the other hand, forgery attempts, that we model by swapping the target register with Haar-randomly generated states, are only rejected with high probability when the parameter μ is set to be sufficiently high, thereby establishing a trade-off.

Alternatively, we approach the problem of distinguishing users from attackers as a binary classification task using DNN. We focus on distinguishing attackers from users by measuring the control register as described in Eq. (3), generating a dataset comprising measurements from $3 \cdot 10^3$ users and $3 \cdot 10^3$ attackers for $\lambda = 100$, with a ratio distribution between the training and validation sets of 0.2.

Given the low amount of data used for the training set compared to the DNN input size $\lambda = 100$, we average every 10 consecutive bits in the DNN input string. This approach balances the trade-off between the DNN's ability to learn from a smaller sample of input data and the potential loss of information due to the disruption of bit relations in the complete $\lambda = 100$ input string.

The deep neural network (DNN) architecture used in this study consists of two hidden layers each with 15 nodes. Each layer employs the rectified linear unit (ReLU) activation function, while the output layer uses the sigmoid activation function. The model is trained using the binary cross-entropy loss function and the Adam optimizer. To determine the optimal hyperparameters (depth and width) for the DNN given a specific λ , we evaluate five different arbitrary configurations of the DNN architecture and select the one that achieves the best performance.

B. Results

1) *Noise impact*: The authentication protocol depicted in Fig. 2 was simulated for various distances d between server and user, ranging from $d \in [0, 10]$ km. After receiving and storing all 5×10^2 photons, the user waits for a time $T \in [0, 15]$ μ s before sending the qubits back to the server.

For each data point in Fig. 2, the mean and variance of r_{01} were calculated by simulating 6 different users. The high values for the variance arise from the low number of photons ($\lambda = 500$) used for each user, which was not set to be

higher because the more photons are considered, the longer the storage times become. More specifically, adding an order of magnitude to λ would lead to storage times of around 150 μ s, resulting in low memory performance ($\eta_{\text{store}} = 0.22$) as well as high qubit dephasing.

In Fig. 2 (left), we can observe that r_{01} slightly decreases as storage times increase up to 15 μ s, while in Fig. 2 (right) r_{01} decreases exponentially, as expected from the fiber loss channel. Specifically, after reaching $d = 5$, r_{01} achieves values close to $\frac{1}{2}$, compatible with those coming from forgery attempts.

2) *User-server protocol performance*: In Fig. 3, we compare two methods for the binary classification problem of distinguishing attackers from users: either using acceptance condition a) or acceptance condition b) (see Section III-B).

For a distance of 10 km and a memory storage time of 1 μ s, we sample a range of values of μ to identify the optimal bound and compare this peak accuracy to that of the DNN. With $\lambda = 100$, the DNN algorithm shows improved performance in the classification task, achieving a correct classification frequency of 0.75. The improvement in performance, compared to the static method, is attributed to the DNN's capability to learn the correlations between bits in the input string.

VI. CONCLUSIONS

In this article we start by providing the reader with a new method for secure user-server authentication under quantum noiseless assumptions. We leverage the properties of maximally entangled pairs within the design of a specific quantum circuit that we split into two stages: generation and verification. Afterwards, we revisit the BB84 QKD protocol in order to add slight modifications to it, allowing for mutual entity authentication. This is first done with the symmetric scheme, in which our user-server scheme is trivially exploited. Later on, we conveniently adapt our proposal in order to diminish the requirements of the scheme. More precisely, what we name the asymmetric scheme requires a unidirectional quantum channel, whereas the symmetric scheme requires a bidirectional one.

In a practical simulation, our user-server authentication protocol is evaluated under noisy channel conditions utilizing AFC cavity-enhanced memories, spanning distances ranging from 1 to 10 km and storage times up to 15 μ s. Feasibility requirements are established, with notable outcomes observed for a 1 km distance and a storage time of 1 μ s, yielding $r_{01} = 0.67 \pm 0.05$. Moreover, a deep neural network (DNN) approach is proposed for binary classification, distinguishing between legitimate users and forgery attempts, achieving a correct classification rate of 0.75 for memory storage times of 1 μ s and a 10 km distance between the user and server parties.

Before concluding the article, we aim to stress that creating a quantum based authentication protocol with computational security remains an open challenge, unless bounds on the amount of noise are heuristically set. In this line, we reckon that our realistic simulation openly tackles the scope of our

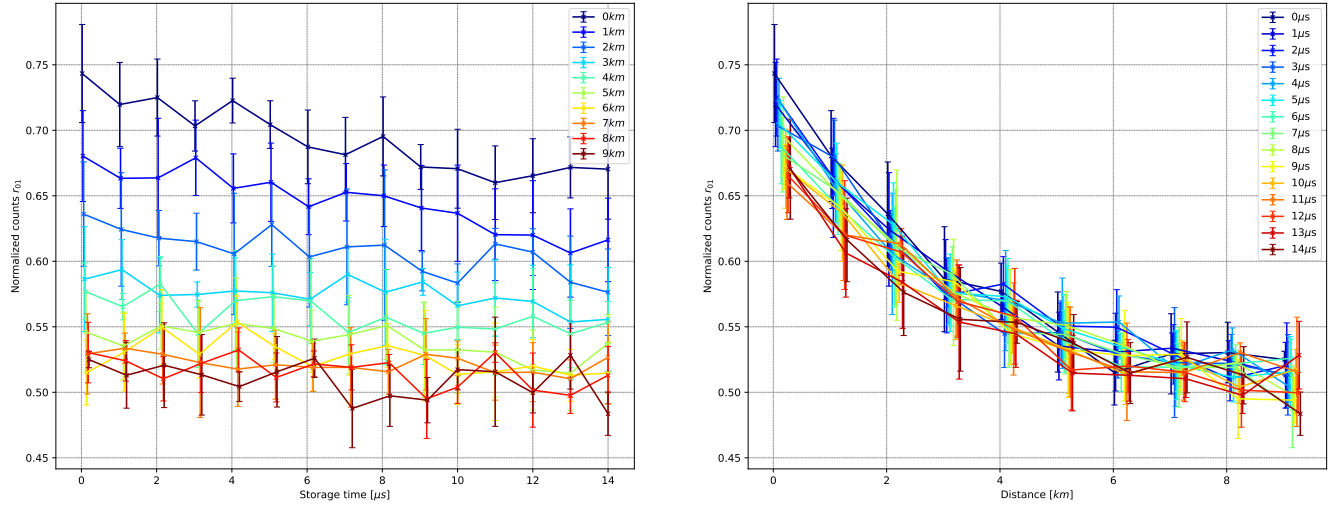


Fig. 2: User-server authentication protocol with the simulation parameters presented in Table I and $\lambda = 500$: Left) r_{01} in terms of storage time for multiple distances. Right) r_{01} in terms of distance for multiple storage times. We have considered one standard deviation for the error-bars creation and we have set an offset in x -axis, so the uncertainty could be easily identified, all values in x -axis should be integers for both plots.

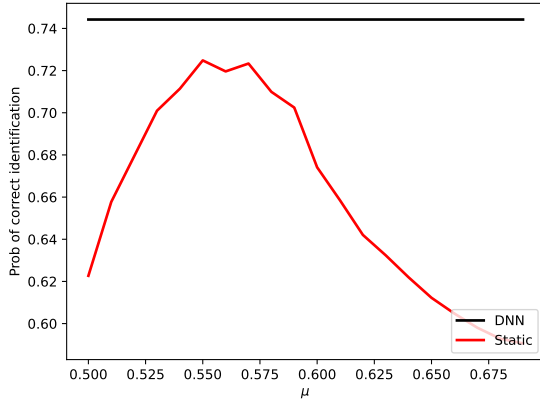


Fig. 3: Relative frequency of correctly distinguishing between users and attackers, with $\lambda = 100$ and for both static and DNN methods.

noiseless derivation, together with providing the reader with deep insights on the state of the art of AFC quantum memories. Future research avenues are suggested, including the incorporation of error correction schemes, consideration of different attack scenarios and exploration of alternative machine learning techniques for classification tasks. For instance, we suggest that a convolutional neural network (CNN) [41] architecture may improve the performance of the binary classification task compared to our DNN, due to the CNN's ability to recognize patterns in extensive matrix input data as shown for image

recognition.

APPENDIX

A. Proofs

Proposition 1. *The noiseless protocol described in Section III is complete.*

Proof. If CX is the chosen gate to be applied in the first stage of the protocol, the state of the "control-target" bipartite system right before the final measurement is

$$|\psi_{\text{pre-meas}}\rangle_{CT} = |0\rangle_C \otimes |1\rangle_T \quad (12)$$

and, thus, such measurement always outputs the classical value "0".

If CZX is chosen instead, the final state takes the form of

$$|\psi_{\text{pre-meas}}\rangle_{CT} = |1\rangle_C \otimes |1\rangle_T \quad (13)$$

and, thus, such measurement always outputs the classical value "1". \square

Proposition 2. *The noiseless protocol described in Section III is sound.*

Proof. At each of the λ rounds involved in the protocol defined in Section III, the attacker needs to send a single qubit as a forgery attempt. As stated in Section II, we model the power limitation of any attacker by simply asking him/her not to own the quantum system the actual user was provided with.

Nonetheless, the attacker may have had access to such quantum system and tampered with it, performing, for instance, joint evolutions with it and another system.

Let us define an auxiliary variable m taking the value 0 if CX is chosen at generation and taking the value 1 otherwise, and let us denote the bipartite state obtained after the generation stage in Eq.3 as $|\psi_{\text{post-gen}}\rangle_{CT}$, so that

$$|\psi_{\text{post-gen}}\rangle_{CT} = \frac{1}{\sqrt{2}} \left(|00\rangle + (-1)^m |11\rangle \right). \quad (14)$$

Additionally, let ρ_A be a density matrix description of a system owned by the attacker and which, generally, will be described as a multiqubit register A. Such density matrix may be jointly evolved with the target party before sending one qubit within ρ_A to the verification stage.

The overall system ρ_{overall} describing both control and target registers, together with the system owned by the attacker after a potential tampering has occurred, can be written as

$$\rho_{\text{overall}} = \mathbb{I}_2 \otimes G_{TA} \left(|\psi_{\text{post-gen}}\rangle_{CT} \langle \psi_{\text{post-gen}}|_{CT} \otimes \rho_A \right), \quad (15)$$

where G_{TA} is an arbitrary unitary evolution acting on both systems T and A.

Notice that $\exists K \in \mathbb{N}$ s.t.

$$G_{TA} = \sum_{i=1}^K G_{T_i} \otimes G_{A_i}, \quad (16)$$

where, respectively and $\forall i$, G_{T_i} and G_{A_i} act on the T and A registers.

Now, by combining Eq. (14), Eq. (15) and Eq. (16), we obtain

$$\begin{aligned} \rho_{\text{overall}} = & \frac{1}{2} \left(|0\rangle_C \langle 0|_C \otimes \sum_{i=1}^K G_{T_i} |0\rangle_T \langle 0|_T G_{T_i}^\dagger \otimes G_{A_i} \rho_A G_{A_i}^\dagger + \right. \\ & + |1\rangle_C \langle 1|_C \otimes \sum_{i=1}^K G_{T_i} |1\rangle_T \langle 1|_T G_{T_i}^\dagger \otimes G_{A_i} \rho_A G_{A_i}^\dagger + \\ & + (-1)^m |0\rangle_C \langle 1|_C \otimes \sum_{i=1}^K G_{T_i} |0\rangle_T \langle 1|_T G_{T_i}^\dagger \otimes G_{A_i} \rho_A G_{A_i}^\dagger + \\ & \left. + (-1)^m |1\rangle_C \langle 0|_C \otimes \sum_{i=1}^K G_{T_i} |1\rangle_T \langle 0|_T G_{T_i}^\dagger \otimes G_{A_i} \rho_A G_{A_i}^\dagger \right). \quad (17) \end{aligned}$$

Finally, when tracing out the target system, and $\forall m$, the following is obtained

$$\text{Tr}_T(\rho_{\text{overall}}) = \frac{1}{2} \mathbb{I}_2 \otimes \rho'_A, \quad (18)$$

where we have defined $\rho'_A \equiv \sum_{i=1}^K G_{A_i} \rho_A G_{A_i}^\dagger$.

Hence, after the specific verification circuit choice and, indeed, after any arbitrary choice, the state obtained at the

control register remains being the maximally mixed state. Therefore, the result "0" is output with probability $\frac{1}{2}$ when measuring the control register and, since each measurement stands for an independent event, the probability p_{f_B} for an attacker to be accepted fulfills

$$p_{f_B} = \frac{1}{2\lambda}. \quad (19)$$

□

Proposition 3. *A forgery attempt against, either our user-server protocol or our symmetric authenticated QKD scheme, aiming to be accepted under acceptance condition a) only succeeds with a probability fulfilling*

$$p(r_{01} \geq \mu) \leq \frac{1}{2\lambda} \frac{1}{\left(\mu - \frac{1}{2}\right)^2} \quad (20)$$

Proof. Proposition 2 serves as a proof that, for an attacker, the probability of obtaining the desired outcome at each round is $\frac{1}{2}$, in both our user-server and authenticated QKD schemes. The measurement at the control register is thus equivalent to a coin toss, with $\frac{1}{2}$ being the expected value of the experiment outcome and $\frac{1}{\sqrt{2}}$ its standard deviation. The central limit theorem [42] together with Chebysev's inequality [43] ensure that the probability of obtaining a rate $r_{01} \geq \mu$ greater or equal than $\mu > \frac{1}{2} + \frac{1}{\sqrt{2\lambda}}$ is

$$p(r_{01} \geq \mu) \leq \frac{1}{2\lambda} \frac{1}{\left(\mu - \frac{1}{2}\right)^2}. \quad (21)$$

□

Proposition 4. *The asymmetric scheme for authenticating the BB84 protocol owns completeness and soundness in a noiseless scenario.*

Proof. Propositions 1 and 2 serve to show how Bob is securely authenticated within the noiseless protocol described in IV-C.

Regarding Alice, the state owned by Bob after carrying out Eq.7 onto half of his entangled pairs is

$$|0\rangle_C \otimes |+\rangle_T \quad (22)$$

where $+$ ($-$) holds when CX (CZX) is chosen at generation.

Thus, he obtains "0" as a classical outcome in the indicated measurement with probability equal to 1.

If the qubits are not sent by Alice, his control register is described as being $\frac{1}{2} \mathbb{I}_2$ and, thus, the probability for an attacker to forge the identity of Alice is equal to

$$p_{f_C} = \frac{1}{2\lambda}. \quad (23)$$

□

B. AFC memory hardware parameters

In Table.II, we deliver an overview of the main hardware parameters and their evolution throughout the past recent years.

TABLE II: Hardware parameters: values overview

Previous works	Comb finesse (F)	Storage time	Absorption coefficient (α)	Storage efficiency
Mikael Afzelius. et al. [44] 2010	2.5	20 μ s	0.5	1%
Mahmood Sabooni et al. [38] 2013	3.0	1.1 μ s	1	(58 \pm 5)%
P Jobez et al. [45] 2014	5.0	2 μ s / 10 μ s	1.2	53%/28%
Jacob H. D. et al. [46] 2020	2.0	25 ns	0.45	27.5%
Yu Ma et al. [28] 2021	2.2	60 min	2.6	0.06% for 5 min storage
Stefano Duranti. et al. [27] 2023	5.8	2 μ s	0.46	62%

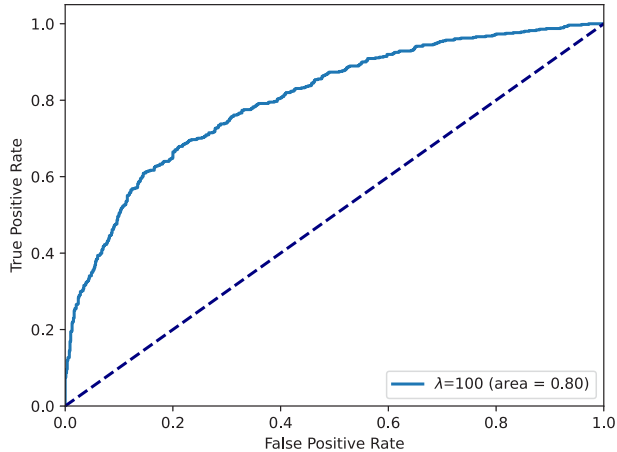


Fig. 4: ROC curve for $\lambda = 100$.

C. Performance of the DNN

D. ROC Curve

The receiver operating characteristic curve (ROC) [47] for the used DNN is shown in Fig. 4.

E. Accuracy and cross entropy loss

The classification accuracy and cross-entropy loss are depicted in Fig. 5. The DNN achieves higher accuracy and lower cross-entropy loss during the training procedure. Fig. 5 justifies the use of only 100 iterations for the DNN training, as we observe that both the cross-entropy loss and accuracy curves have stabilized by then.

CODE AVAILABILITY

All codes responsible for the results in this article can be found at: <https://github.com/terrordayvg/Quantum authentication>.

ACKNOWLEDGEMENTS

CD, VG, and JN acknowledge the financial support by the Federal Ministry of Education and Research of Germany in the programme of “Souverän. Digital. Vernetzt”. Joint project 6G-life, project identification number: 16KISK002. Furthermore, VG and JN acknowledge the financial support under projects 16KISQ039 and 16KISQ077 and by the DFG via project NO 1129/2-1. CD was further supported under projects 16KISQ077, 16KISQ037, 16KISR026, 16KIS1598, and 16KISQ093.

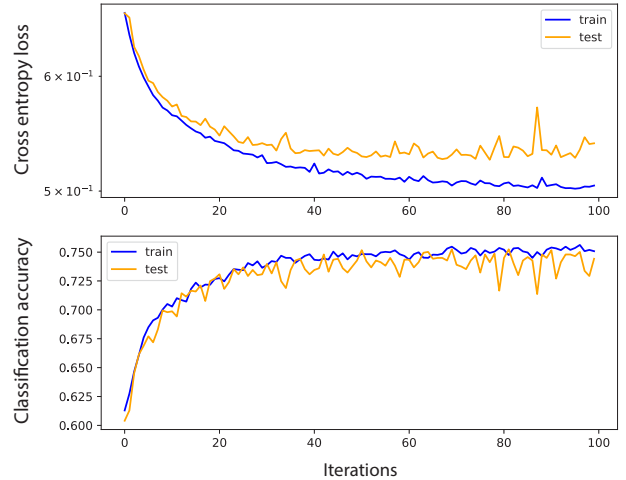


Fig. 5: Accuracy and cross entropy for the training and test set of $\lambda = 100$ for the DNN, for distance of 10 km and storage time of 1 μ s.

REFERENCES

- [1] C. Bennett and G. Brassard, “Withdrawn: Quantum cryptography: Public key distribution and coin tossing,” vol. 560, 01 1984, pp. 175–179.
- [2] A. K. Ekert, “Quantum cryptography based on bell’s theorem,” *Phys. Rev. Lett.*, vol. 67, pp. 661–663, Aug 1991. [Online]. Available: <https://link.aps.org/doi/10.1103/PhysRevLett.67.661>
- [3] N. Sharma, P. Singh, A. Anand, S. K. Chawla, A. K. Jain, and V. Kukreja, *A Review on Quantum Key Distribution Protocols, Challenges, and Its Applications*, 03 2024, pp. 541–550.
- [4] A. I. Nurhadi and N. R. Syambas, “Quantum key distribution (qkd) protocols: A survey,” in *2018 4th International Conference on Wireless and Telematics (ICWT)*, 2018, pp. 1–5.
- [5] A. Garcia-Callejo, A. Ruiz-Chamorro, D. Cano, and V. Fernandez, “A review on continuous-variable quantum key distribution security,” in *Proceedings of the International Conference on Ubiquitous Computing & Ambient Intelligence (UCAmI 2022)*, J. Bravo, S. Ochoa, and J. Favela, Eds. Cham: Springer International Publishing, 2023, pp. 1073–1085.
- [6] A. Dutta and A. Pathak, “A short review on quantum identity authentication protocols: How would bob know that he is talking with alice?” 2021.
- [7] B. Skoric, “Quantum readout of physical unclonable functions: Remote authentication without trusted readers and authenticated quantum key exchange without initial shared secrets,” *Cryptology ePrint Archive*, Paper 2009/369, 2009, <https://eprint.iacr.org/2009/369>. [Online]. Available: <https://eprint.iacr.org/2009/369>
- [8] M. Arapinis, M. Delavar, M. Doosti, and E. Kashefi, “Quantum physical unclonable functions: Possibilities and impossibilities,” *Quantum*, vol. 5, p. 475, Jun. 2021. [Online]. Available: <http://dx.doi.org/10.22331/q-2021-06-15-475>
- [9] S. Ghosh, V. Galetsky, P. J. Farré, C. Deppe, R. Ferrara, and H. Boche, “Existential Unforgeability in Quantum Authentication From Quantum Physical Unclonable Functions Based on Random von Neumann Measurement,” 4 2024.

- [10] H. Park, B. K. Park, M. Woo, M.-S. Kang, J.-W. Choi, J.-S. Kang, Y. Yeom, and S.-W. Han, "Mutual entity authentication of quantum key distribution network system using authentication qubits," *EPJ Quantum Technology*, vol. 10, 11 2023.
- [11] S. Rass, S. König, and S. Schauer, "Bb84 quantum key distribution with intrinsic authentication," in *ICQNM 2015*, 2015, pp. 41–44, the Ninth International Conference on Quantum, Nano/Bio, and Micro Technologies (ICQNM 2015) ; Conference date: 23-08-2015 Through 28-08-2015.
- [12] S. Aaronson and P. Christiano, "Quantum money from hidden subspaces," 2012.
- [13] S. Jasim, O. Kamil, and N. Alhyani, "A review of jamming attacks in wireless systems," vol. 8, pp. 16–22, 02 2023.
- [14] V. Sze, Y.-H. Chen, T.-J. Yang, and J. Emer, "Efficient processing of deep neural networks: A tutorial and survey," 2017.
- [15] P. W. Shor and J. Preskill, "Simple proof of security of the bb84 quantum key distribution protocol," *Physical Review Letters*, vol. 85, no. 2, p. 441–444, Jul. 2000. [Online]. Available: <http://dx.doi.org/10.1103/PhysRevLett.85.441>
- [16] D. Elkouss, J. Martinez-Mateo, and V. Martin, "Information reconciliation for quantum key distribution," 2011.
- [17] S. Watanabe, R. Matsumoto, and R. Uyematsu, "Noise tolerance of the bb84 protocol with random privacy amplification," in *Proceedings. International Symposium on Information Theory, 2005. ISIT 2005.*, 2005, pp. 1013–1017.
- [18] D. Javeed and U. MohammedBadamasi, "Man in the middle attacks: Analysis, motivation and prevention," *International Journal of Computer Networks and Communications Security*, vol. 8, pp. 52–58, 07 2020.
- [19] C. Lee, I. Sohn, and W. Lee, "Eavesdropping detection in bb84 quantum key distribution protocols," *IEEE Transactions on Network and Service Management*, vol. 19, no. 3, pp. 2689–2701, 2022.
- [20] M. Semplicio, B. Oliveira, C. Margi, P. Barreto, T. Carvalho, and M. Naslund, "Survey and comparison of message authentication solutions on wireless sensor networks," *Ad Hoc Networks*, vol. 11, pp. 1221 – 1236, 05 2013.
- [21] G. Zeng and X. Wang, "Quantum key distribution with authentication," 12 1998.
- [22] L. G. Pierson and P. J. Robertson, "Authentication without secrets," 11 2015. [Online]. Available: <https://www.osti.gov/biblio/1226788>
- [23] H. Abdullah, M. Alrawi, and D. Hammod, "Message authentication using new hash function," *Journal of Al-Nahrain University-Science*, vol. 19, pp. 148–153, 09 2016.
- [24] J. L. Carter and M. N. Wegman, "Universal classes of hash functions," in *Proceedings of the ninth annual ACM symposium on Theory of computing*. ACM, 1977, pp. 106–112.
- [25] A. Abidin, "Authentication in quantum key distribution : Security proof and universal hash functions," 2013. [Online]. Available: <https://api.semanticscholar.org/CorpusID:14078938>
- [26] Michael M. McKerns, Leif Strand, Tim Sullivan, Alta Fang, and Michael A.G. Aivazis, "Building a Framework for Predictive Science," in *Proceedings of the 10th Python in Science Conference*, Stéfan van der Walt and Jarrod Millman, Eds., 2011, pp. 76 – 86.
- [27] S. Duranti, S. Wengerowsky, L. Feldmann, A. Seri, B. Casabone, and H. de Riedmatten, "Efficient cavity-assisted storage of photonic qubits in a solid-state quantum memory," 2023.
- [28] Y. Ma, Y.-Z. Ma, Z.-Q. Zhou, C.-F. Li, and G.-C. Guo, "One-hour coherent optical storage in an atomic frequency comb memory," *Nature Communications*, vol. 12, no. 1, p. 2381, Apr 2021. [Online]. Available: <https://doi.org/10.1038/s41467-021-22706-y>
- [29] S. P. Horvath, M. K. Alqedra, A. Kinos, A. Walther, J. M. Dahlström, S. Kröll, and L. Rippe, "Noise-free on-demand atomic frequency comb quantum memory," *Phys. Rev. Res.*, vol. 3, p. 023099, May 2021. [Online]. Available: <https://link.aps.org/doi/10.1103/PhysRevResearch.3.023099>
- [30] A. Seri, D. Lago-Rivera, A. Lenhard, G. Corrielli, R. Osellame, M. Mazzera, and H. de Riedmatten, "Quantum storage of frequency-multiplexed heralded single photons," *Phys. Rev. Lett.*, vol. 123, p. 080502, Aug 2019. [Online]. Available: <https://link.aps.org/doi/10.1103/PhysRevLett.123.080502>
- [31] M. Bonarota, J.-L. L. Gouët, and T. Chanelière, "Highly multimode storage in a crystal," *New Journal of Physics*, vol. 13, no. 1, p. 013013, jan 2011. [Online]. Available: <https://dx.doi.org/10.1088/1367-2630/13/1/013013>
- [32] P. Jobez, N. Timoney, C. Laplane, J. Etesse, A. Ferrier, P. Goldner, N. Gisin, and M. Afzelius, "Towards highly multimode optical quantum memory for quantum repeaters," *Phys. Rev. A*, vol. 93, p. 032327, Mar 2016. [Online]. Available: <https://link.aps.org/doi/10.1103/PhysRevA.93.032327>
- [33] A. Ortu, J. V. Rakonjac, A. Holzäpfel, A. Seri, S. Grandi, M. Mazzera, H. de Riedmatten, and M. Afzelius, "Multimode capacity of atomic-frequency comb quantum memories," *Quantum Science and Technology*, vol. 7, no. 3, p. 035024, Jun. 2022. [Online]. Available: <http://dx.doi.org/10.1088/2058-9565/ac73b0>
- [34] X. Liu, J. Hu, Z.-F. Li, X. Li, P.-Y. Li, P.-J. Liang, Z.-Q. Zhou, C.-F. Li, and G.-C. Guo, "Heralded entanglement distribution between two absorptive quantum memories," *Nature*, vol. 594, no. 7861, pp. 41–45, Jun 2021. [Online]. Available: <https://doi.org/10.1038/s41586-021-03505-3>
- [35] M. Rančić, M. P. Hedges, R. L. Ahlefeldt, and M. J. Sellars, "Coherence time of over a second in a telecom-compatible quantum memory storage material," *Nature Physics*, vol. 14, no. 1, pp. 50–54, Jan 2018. [Online]. Available: <https://doi.org/10.1038/nphys4254>
- [36] T. Coopmans, R. Kneijens, A. Dahlberg, D. Maier, L. Nijsten, J. de Oliveira Filho, M. Papendrecht, J. Rabbie, F. Rozpkedek, M. Skrzypczyk, L. Wubben, W. de Jong, D. Podareanu, A. Torres-Knoop, D. Elkouss, and S. Wehner, "Netsquid, a network simulator for quantum information using discrete events," *Communications Physics*, vol. 4, no. 1, p. 164, Jul 2021. [Online]. Available: <https://doi.org/10.1038/s42005-021-00647-8>
- [37] M. Afzelius, C. Simon, H. de Riedmatten, and N. Gisin, "Multimode quantum memory based on atomic frequency combs," *Phys. Rev. A*, vol. 79, p. 052329, May 2009. [Online]. Available: <https://link.aps.org/doi/10.1103/PhysRevA.79.052329>
- [38] M. Sabooni, Q. Li, S. Kröll, and L. Rippe, "Efficient quantum memory using a weakly absorbing sample," *Phys. Rev. Lett.*, vol. 110, p. 133604, Mar 2013. [Online]. Available: <https://link.aps.org/doi/10.1103/PhysRevLett.110.133604>
- [39] M. Afzelius and C. Simon, "Impedance-matched cavity quantum memory," *Phys. Rev. A*, vol. 82, p. 022310, Aug 2010. [Online]. Available: <https://link.aps.org/doi/10.1103/PhysRevA.82.022310>
- [40] L. Ma, O. Slattery, and X. Tang, "Single photon frequency up-conversion and its applications," *Physics Reports*, vol. 521, no. 2, pp. 69–94, 2012, single photon frequency up-conversion and its applications. [Online]. Available: <https://www.sciencedirect.com/science/article/pii/S0370157312002384>
- [41] R. Yamashita, M. Nishio, R. K. G. Do, and K. Togashi, "Convolutional neural networks: an overview and application in radiology," *Insights into Imaging*, vol. 9, no. 4, pp. 611–629, Aug 2018. [Online]. Available: <https://doi.org/10.1007/s13244-018-0639-9>
- [42] S. Kwak and J. Kim, "Central limit theorem: The cornerstone of modern statistics," *Korean Journal of Anesthesiology*, vol. 70, p. 144, 04 2017.
- [43] G. Alsmeyer, *Chebyshev's Inequality*, 01 2011, pp. 239–240.
- [44] A. Amari, A. Walther, M. Sabooni, M. Huang, S. Kröll, M. Afzelius, I. Usmani, B. Lauritzen, N. Sangouard, H. de Riedmatten, and N. Gisin, "Towards an efficient atomic frequency comb quantum memory," *Journal of Luminescence*, vol. 130, no. 9, pp. 1579–1585, 2010, special Issue based on the Proceedings of the Tenth International Meeting on Hole Burning, Single Molecule, and Related Spectroscopies: Science and Applications (HBSM 2009) - Issue dedicated to Ivan Lorgere and Oliver Guillot-Noel. [Online]. Available: <https://www.sciencedirect.com/science/article/pii/S0022231310000220>
- [45] P. Jobez, I. Usmani, N. Timoney, C. Laplane, N. Gisin, and M. Afzelius, "Cavity-enhanced storage in an optical spin-wave memory," *New Journal of Physics*, vol. 16, no. 8, p. 083005, aug 2014. [Online]. Available: <https://dx.doi.org/10.1088/1367-2630/16/8/083005>
- [46] J. H. Davidson, P. Lefebvre, J. Zhang, D. Oblak, and W. Tittel, "Improved light-matter interaction for storage of quantum states of light in a thulium-doped crystal cavity," *Phys. Rev. A*, vol. 101, p. 042333, Apr 2020. [Online]. Available: <https://link.aps.org/doi/10.1103/PhysRevA.101.042333>
- [47] T. Fawcett, "Introduction to roc analysis," *Pattern Recognition Letters*, vol. 27, pp. 861–874, 06 2006.